Modeling a Slotted Multiband Gasket Monopole Antenna Using NEC

Steven R. Best
AFRL/SNHA
80 Scott Drive
Hanscom AFB, MA 01731
steven.best@verizon.net

Jarrett D. Morrow
Cushcraft Corporation
48 Perimeter Road
Manchester, NH 03103
jarrettm@cushcraft.com

Abstract: In this paper, a solid plate, slotted, multiband gasket monopole antenna is modeled using NEC with a wire grid approximation of the plate structure. The objective of this work is to determine the extent and accuracy to which the wire grid NEC model can predict the resonant frequencies, the anti-resonant frequencies, and the impedance of the multiband gasket. The NEC simulated return loss and impedance are compared with measured data and FDTD simulations performed using CST's Microwave Studio (MWS). Results show that the wire grid NEC model can be used to accurately predict the return loss properties of the antenna including its operating frequencies of minimum return loss. It is also shown that the wire grid NEC model can very accurately predict the antenna's resonant and anti-resonant frequencies, and the corresponding resistance.

Keywords: Multiband Antennas, Monopole Antennas, Numerical Modeling

1. The Slotted Multiband Gasket Monopole

The slotted gasket monopole antenna considered here is derived from a Sierpinksi gasket monopole and has previously been shown to exhibit multiband behavior [1]. The solid plate, slotted, gasket monopole antenna is shown in Fig. 1. The antenna is 15.24 cm in height and was fabricated using 0.0508 cm brass sheet stock. The four slots were milled and located at heights of 0.95 cm, 1.91 cm, 3.81 cm, and 7.62 cm. For measurement purposes the antenna was mounted over a 120 cm by 120 cm aluminum ground plane and was base fed with an SMA panel mount connector. The antenna impedance was measured over a frequency spectrum of 50 MHz through 12 GHz. The measured return loss of the antenna is presented Fig. 2. The return loss is determined relative to an impedance of 50 Ohms and illustrates the antenna's multiband behavior. Over the frequency spectrum of 50 MHz through 12 GHz, there are 5 well defined frequency ranges of minimum return loss as detailed in Table I.

Table I. Minimum Return Loss Properties of the Slotted Gasket Monopole

Frequency (MHz)	|S11| (dB)
321	-8.3
1148	-19.7
2378	-28.8
4897	-44.6
11313	-38.2

Report Documentation Page

Form Approved
OMB No. 0704-0188

1. REPORT DATE **23 APR 2004**	2. REPORT TYPE **N/A**	3. DATES COVERED **-**

4. TITLE AND SUBTITLE **Modeling a Slotted Multiband Gasket Monopole Antenna Using NEC**	5a. CONTRACT NUMBER
	5b. GRANT NUMBER
	5c. PROGRAM ELEMENT NUMBER
6. AUTHOR(S)	5d. PROJECT NUMBER
	5e. TASK NUMBER
	5f. WORK UNIT NUMBER
7. PERFORMING ORGANIZATION NAME(S) AND ADDRESS(ES) **AFRL/SNHA 80 Scott Drive Hanscom AFB, MA 01731**	8. PERFORMING ORGANIZATION REPORT NUMBER
9. SPONSORING/MONITORING AGENCY NAME(S) AND ADDRESS(ES)	10. SPONSOR/MONITOR’S ACRONYM(S)
	11. SPONSOR/MONITOR’S REPORT NUMBER(S)

12. DISTRIBUTION/AVAILABILITY STATEMENT
Approved for public release, distribution unlimited

13. SUPPLEMENTARY NOTES
See also ADM001763, Annual Review of Progress in Applied Computational Electromagnetics (20th) Held in Syracuse, NY on 19-23 April 2004., The original document contains color images.

14. ABSTRACT

15. SUBJECT TERMS

16. SECURITY CLASSIFICATION OF:			17. LIMITATION OF ABSTRACT	18. NUMBER OF PAGES	19a. NAME OF RESPONSIBLE PERSON
a. REPORT **unclassified**	b. ABSTRACT **unclassified**	c. THIS PAGE **unclassified**	**UU**	**5**	

Standard Form 298 (Rev. 8-98)
Prescribed by ANSI Std Z39-18

2. The NEC Wire Grid Model: Return Loss Properties

The four slots located along the vertical axis of the slotted gasket antenna define its multiband behavior. At each of the operating bands, the maximum surface current density occurs near the narrow metal strips between the slot and edge of the monopole as illustrated in Fig. 3. At a frequency near 1148 MHz, the maximum current density occurs at the edge of the upper most slot, while at a frequency near 11.313 GHz, the maximum current density occurs at the edge of the lowest slot. The challenge in constructing a wire grid model of this antenna is ensuring that the wire grid structure in these narrow metal regions, and near the feed point, is sufficiently dense enough so that the high surface current density in these regions of the antenna can be modeled accurately. At the same time, the wire grid must also be sufficient throughout the remainder of the plate structure so that the total surface current density throughout the entire antenna can be modeled accurately.

The NEC wire grid model of the slotted gasket monopole antenna has 7,864 wires and is depicted in Fig. 4. A FORTRAN program was written to create the wire model with the antenna height, top width, slot locations and wire density being arbitrarily set by the user. The slots in this model are located at heights of approximately 0.92 cm, 1.83 cm, 3.81 cm, and 7.5 cm, which are all within 1 to 2 mm of the values in the fabricated antenna. In the wire grid model, the wire density is increased in the lower region of the antenna surrounding the four slots, while it is decreased in the upper region of the antenna where the surface current density is relatively low. The wire diameter in the model is 0.2 mm, the longest wire is 6.097 mm, the shortest wire is 1.524 mm and the closest parallel wire spacing is 0.88 mm. These values were not modified over any part of the frequency spectrum where the wavelength ranges from approximately 6 m to 2.5 cm.

The impedance of the wire grid slotted gasket antenna was calculated using the NEC 4 engine in EZNEC Pro [2] and MWS [3] over a frequency range of 50 MHz through 12 GHz. The FDTD model of the gasket antenna is the solid plate gasket as shown in Fig. 1. In each simulation, the antenna is base fed and mounted over an infinite, perfectly conducting ground plane. The simulated return loss of the slotted gasket antenna is compared with the measured return loss in Fig. 5. Examining the return loss data, the agreement between the NEC and MWS simulations over the entire frequency spectrum is notably remarkable considering the significant differences in which the structures are constructed and numerically modeled within each simulation. There is also very reasonable agreement between the simulated and measured return loss. The only significant point to note is that the MWS FDTD simulation predicts a much lower return loss in the first operating band relative to the values predicted by NEC and measured.

3. The NEC Wire Grid Model: Impedance Properties

With the very good agreement between the simulated and measured return loss of the antenna, one would expect similar agreement between the simulated and measured impedance. A comparison of the simulated and measured impedance is presented in Fig. 6. At low frequencies and through the middle of the frequency spectrum, there is very good agreement between the impedance as predicted by the NEC and MWS simulations. At higher frequencies beyond the middle of the frequency spectrum, the simulated impedances exhibit similar behavior but there is a notable difference in the predicted anti-resonant frequencies near 7 to 8 GHz.

The agreement between the simulated and measured impedance is less than marginal. At the low end of the frequency spectrum, there is good agreement between the simulated and measured resonant frequencies ($dX/dw > 0$) and impedance. However, the first simulated and measured anti-resonant frequencies ($dX/dw < 0$) are not in good agreement. The first simulated anti-resonant frequency is approximately 700 MHz, while the first measured anti-resonant frequency is approximately 525 MHz. One might conclude that the simulations do not accurately predict the anti-resonant frequencies and impedance of the actual antenna. With the very good agreement between the simulated and measured return loss properties this is unlikely to be the case.

At a frequency near 3.4 GHz, the NEC simulation predicts an anti-resonance and a resistance of approximately 226 O. At the same frequency, the measured impedance is near a resonance and the resistance is very low at approximately 15 O. This relative difference in impedance is indicative of a difference in the reference planes of the simulation feed point location and the measurement feed point location, which is established by the measurement calibration process. A shift in the relative feed point reference planes affects the location of the anti-resonant frequencies more so than the resonant frequencies because in the frequency ranges near anti-resonance, the magnitude of the impedance is significantly greater than it is near resonance.

Since the measurement feed point reference plane is established by the measurement calibration process, we can adjust this reference plane to more closely match that established by the feed point location in the simulations. This can be accomplished by adding electrical delay to the measured impedance to align one of the anti-resonant frequencies. If, in fact, a shift in the feed point reference planes is the primary factor causing the difference between the simulated and measured impedance, shifting the measurement reference plane should correct the measured impedance over the entire frequency spectrum. For instance, the NEC simulation predicts an anti-resonant frequency at 3.415 GHz, with a resistance of 227.6 O. The measured impedance at this frequency is 15.5 – j19.9 O. Shifting this impedance to anti-resonance with an electrical delay of approximately 66.5°, the measured impedance is anti-resonant with a resistance of 189 O, which is significantly closer to the simulated impedance. Applying the equivalent electrical delay to the entire spectrum, the feed point reference plane of the measured impedance is adjusted to match that of the simulation. A comparison of the NEC simulated impedance and the measured impedance with a shifted reference plane is presented in Fig. 7.

From Fig. 7 it can be seen that there is very good agreement between the NEC simulated and shifted measured impedance over the frequency spectrum through approximately 8 GHz. At the lower frequencies, both the resonant and anti-resonant behavior of the antenna are simulated with very good accuracy. At the higher frequencies, the simulated and measured impedance exhibit similar behavior. At these higher frequencies, lesser agreement between the simulation and measurement might be expected due to the nature of the wire grid model and the smaller wavelengths. However, with the very good agreement between the NEC and MWS simulated return loss at these frequencies, it also possible that there is an issue with the measured data. Finally, it should noted that the difference between the NEC and MWS simulated impedance at the higher frequencies is likely a result of different feed point reference planes in the two simulations.

References

[1] S. R. Best, “A multiband conical monopole antenna,” *IEEE Antenna Wireless Propag. Letters*, Vol. 2, pp. 205-207, 2003.
[2] EZNEC Pro, Roy Lewallen, www.eznec.com
[3] Micro Wave Studio, Computer Simulation Technologies, www.cst.de

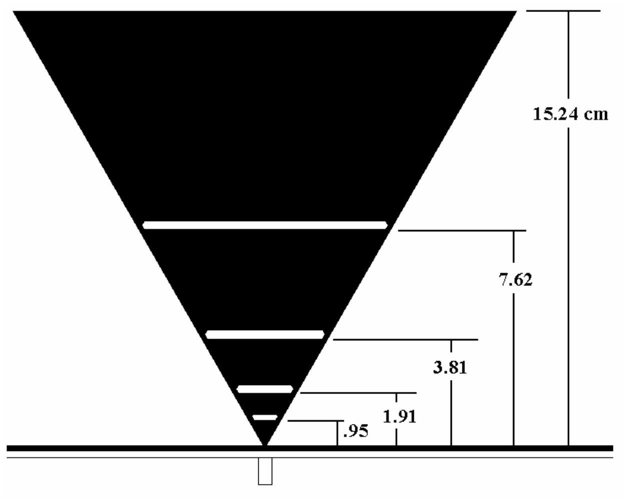

Fig. 1. The solid plate, slotted, multiband gasket monopole antenna.

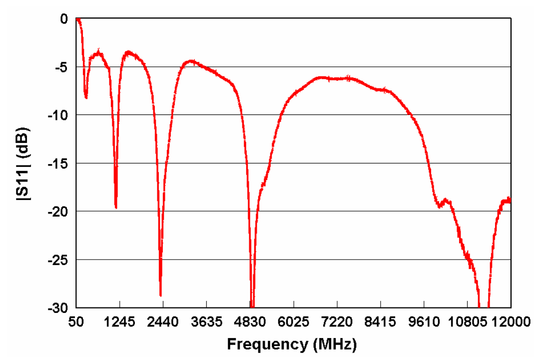

Fig. 2. Measured return loss of the slotted, multiband gasket monopole antenna relative to 50 Ohms impedance.

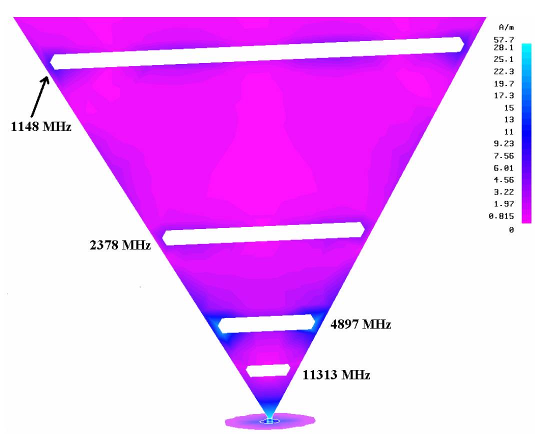

Fig. 3. Current concentration points along the slotted gasket monopole as a function of operating band. The surface current distribution is shown for a frequency of 4897 MHz.

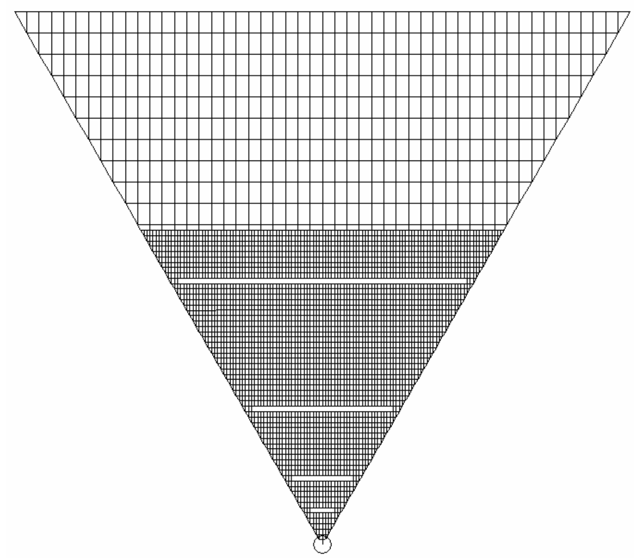

Fig. 4. NEC wire grid layout of the slotted, multiband gasket antenna containing 7,864 wires.

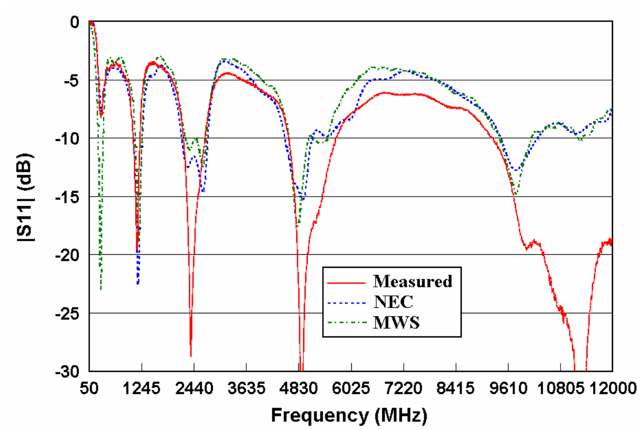

Fig. 5. A comparison of the simulated and measured return loss of the slotted, multiband gasket monopole antenna.

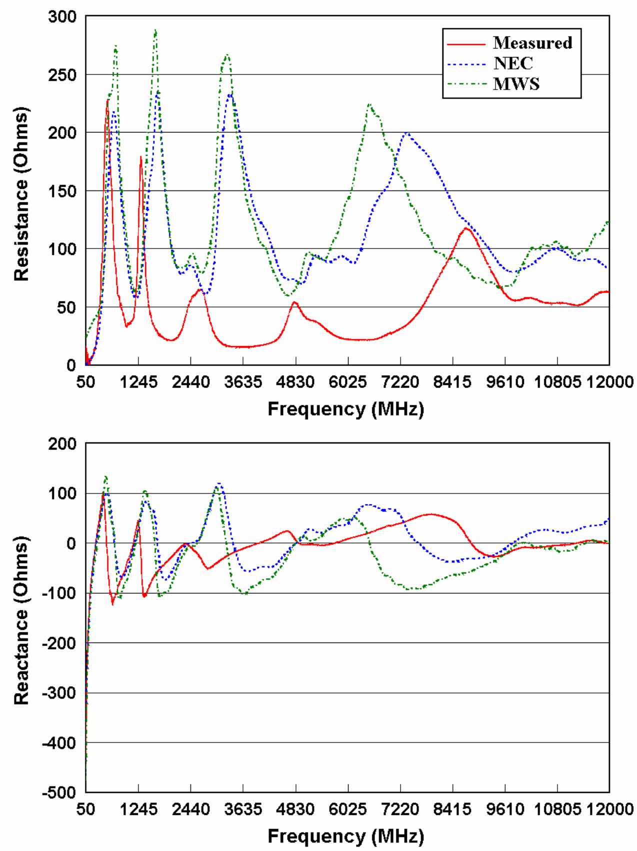

Fig. 6. A comparison of the simulated and measured impedance data over a frequency spectrum of 50 MHz through 12 GHz.

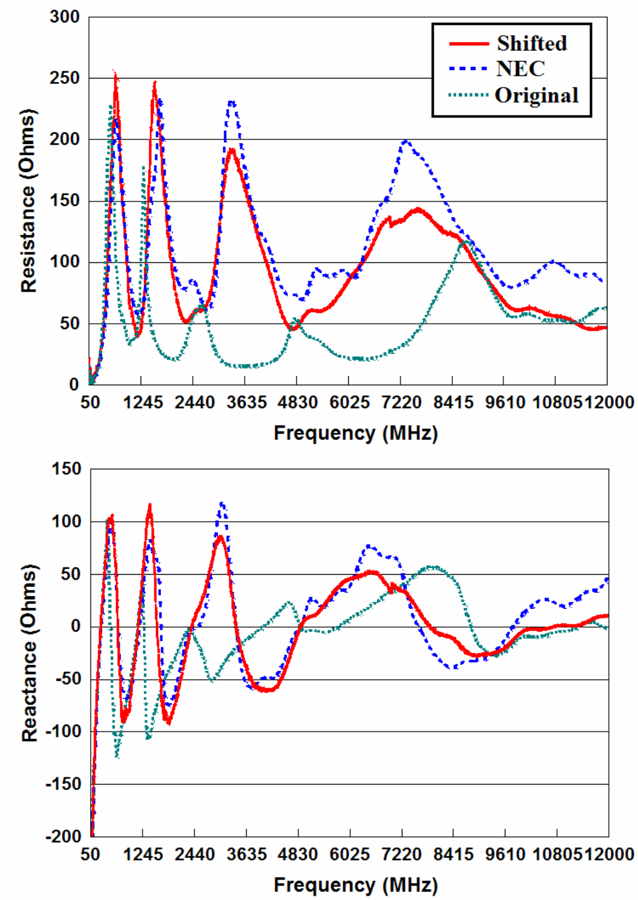

Fig. 7. A comparison of the simulated and measured impedance data over a frequency spectrum of 50 MHz through 12 GHz. The measured impedance data has been shifted to align the feed point reference planes between the NEC simulation and the measurements.

